Dispersion in the Surfzone: Tracer Dispersion Studies

Dr. Falk Feddersen
Scripps Institutions of Oceanography
IOD/SIO/UCSD 0209, 9500 Gilman Drive, La Jolla CA 92093-0209
858.534.4345, 858.534.0300 (FAX), falk@coast.ucsd.edu
http://iod.ucsd.edu/∼falk

Award Number: N00014-06-1-0330

LONG-TERM GOALS

Terrestrial runoff and river input dominates urban pollutant loading rates Often draining directly into the surfzone, this pollution degrades surfzone water quality, leading to beach closures (*e.g., Boehm et al.*, 2002), increases health risks (*e.g.,* diarrhea and upper respiratory illness) (*Haile et al.*, 1999), and contains both human viruses (*Jiang and Chu*, 2004) and elevated levels of fecal indicator bacteria (*Reeves et al.*, 2004). Surfzone mixing processes disperse and dilute such (and other types of) pollution. On smaller length-scales (smaller than the water depth), breaking-waves and bed-generated turbulence mix tracer. However, field surfzone observations of turbulence previously have been extremely scarce, and much about surfzone small-scale turbulence is not known. On larger scales (10–100 m), horizontal dispersion is driven by surfzone eddies and meanders associated with shear waves (*Oltman-Shay et al.*, 1989) or finite breaking crest length (*Peregrine*, 1998). Understanding the small and large length-scale mixing processes important to predicting the fate (transport, dispersal, and dilution) of surfzone tracers whether pollution, bacteria, larvae, or nutrients.

OBJECTIVES

The scientific objective is to improve understanding and modeling of dispersion of tracers (pollution, fecal indicator bacteria, fine sediments) within the nearshore (a few 100 m of the shoreline) and especially within the surfzone where breaking waves intensify mixing processes and drive strong mean currents. Here the focus is on two components of the analysis of the HB06 experiment performed in Fall of 2006. The first is analysis of surfzone cross-shore dye tracer dispersion (*Clark et al.*, 2009b). The second is studying the small-scale turbulence in the surfzone due to breaking waves. Other HB06 efforts include analysis of surfzone drifter dispersion (*Spydell et al.*, 2009) and phytoplankton patchiness (*Omand et al.*, 2009b).

APPROACH

HB06 Dye Dispersion

Report Documentation Page

Form Approved
OMB No. 0704-0188

1. REPORT DATE **2009**	2. REPORT TYPE	3. DATES COVERED **00-00-2009 to 00-00-2009**
4. TITLE AND SUBTITLE **Dispersion in the Surfzone: Tracer Dispersion Studies**		5a. CONTRACT NUMBER 5b. GRANT NUMBER 5c. PROGRAM ELEMENT NUMBER
6. AUTHOR(S)		5d. PROJECT NUMBER 5e. TASK NUMBER 5f. WORK UNIT NUMBER
7. PERFORMING ORGANIZATION NAME(S) AND ADDRESS(ES) **University of California San Diego,Scripps Institutions of Oceanography,9500 Gilman Drive,La Jolla,CA,92093-0209**		8. PERFORMING ORGANIZATION REPORT NUMBER
9. SPONSORING/MONITORING AGENCY NAME(S) AND ADDRESS(ES)		10. SPONSOR/MONITOR'S ACRONYM(S) 11. SPONSOR/MONITOR'S REPORT NUMBER(S)
12. DISTRIBUTION/AVAILABILITY STATEMENT **Approved for public release; distribution unlimited**		
13. SUPPLEMENTARY NOTES		
14. ABSTRACT		
15. SUBJECT TERMS		

16. SECURITY CLASSIFICATION OF:			17. LIMITATION OF ABSTRACT	18. NUMBER OF PAGES	19a. NAME OF RESPONSIBLE PERSON
a. REPORT **unclassified**	b. ABSTRACT **unclassified**	c. THIS PAGE **unclassified**	**Same as Report (SAR)**	**10**	

Standard Form 298 (Rev. 8-98)
Prescribed by ANSI Std Z39-18

Previous surfzone dye observations have been limited to discrete shoreline or single swimmer bottle samples without measuring the waves and currents (*e.g., Inman et al.*, 1971; *Clarke et al.*, 2007) A newly developed ONR-funded GPS equipped jetski based sampling system (*Clark et al.*, 2009a) was used to create near-synoptic maps of surfzone dye (Rhodamine WT) on six days (denoted R1–R6) during HB06 (*Clark et al.*, 2009b). Dye tracer, released relatively close to the shoreline, was transported alongshore by the alongshore current and dispersed in the cross-shore in a manner resembling a wall-bounded turbulent plume, analogous to a smokestack plume, with axis parallel to the shoreline (*Clark et al.*, 2009b).

Surfzone Turbulent Dissipation Rate:

The vertical structure of turbulence in the surfzone is of interest. Both breaking waves and near-sea-bed shear are possible sources of turbulence. Here a key turbulence statistic, the turbulent dissipation rate ϵ is estimated from Acoustic Doppler Velocimeters observations following *Feddersen et al.* (2007).

WORK COMPLETED

- *Spydell et al.* (2009) was submitted to JGR Oceans in Jan 2009 and was published this summer. This manuscript reported on HB06 drifter observations
- *Omand et al.* (2009) and *Clark et al.* (2009a) have both been published. These manuscripts dealt with the technical details of making Chlorophyll and Rhodamine WT dye observations in the surfzone.
- A manuscript (*Clark et al.*, 2009b) of the HB06 dye dispersion studies has been submitted to JGR Oceans.
- A manuscript (*Omand et al.*, 2009b), reporting on the evolution and dynamics of a nearshore red tide observed during HB06, is near submission.
- A manuscript intended for *J. Atmospheric and Oceanic Tech.* (Feddersen) is almost ready for submission. This manuscript deals with the methods of analyzing Acoustic Doppler Velocimeter data for estimating the turbulent dissipation rate. manuscript looks at surfzone drifter dispersion from Huntington Beach.
- Preparations for the IB09 (Imperial Beach CA in Sept-Oct 2009) experiment have been completed and the IB09 experiment is currently under way.

RESULTS

HB06 Experiment

Observations were collected from 15 September to 17 October 2006 (800 hours) at Huntington Beach CA ,a site with chronic water quality problems. A cross-shore transect of co-located

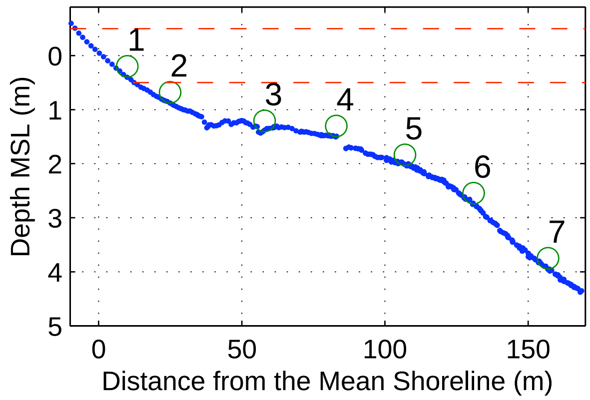

Figure 1: HB06 cross-shore instrument transect. The circled numbers indicate instrumented frames with acoustic Doppler Velocimeters (ADV) and pressure sensors. The horizontal red dashed lines indicate the typical tide range.

pressure sensors and acoustic Doppler Velocimeters was deployed spanning 160 m out to 4 m mean water depth (Fig. 1). The tide range was nominally ± 1 m. The data was sampled at 8 Hz. The ADVs sampled between 0.5-1.0 m above the bed. The cross- and alongshore coordinate are x and y, respectively. The mean water depth is given by h and the vertical coordinate is z with $z = 0$ m at the sea-bed. The distance below the mean sea surface is $z' = h - z$. At each of the frames, hourly estimates of significant wave height H_{sig}, cross-shore energy flux $F = Ec_g$, mean alongshore current $\bar{v}_m$, and turbulent dissipation rate ϵ were estimated.

HB06 Dye Dispersion Observations

The mean cross-shore tracer profiles $\overline{D}(x, y_j)$ average over stirring and meandering (Fig 2) On all releases except R5, the initially narrow $\overline{D}(x, y_j)$ profiles disperse across the surfzone and peak concentrations decrease with downstream distance (increasing y) from the source (Fig 2). During most releases (R2, R3, R4, R6), mean profiles $\overline{D}(x, y_j)$ are shoreline attached with maxima at or near the shoreline (Fig 2). An exception is release R1 which has maxima in the mid to outer surfzone (Fig 2a), which is likely the result of dye released in the mid- to outer-surfzone ($x_0 = -55$ m), and the shortest y_j. Release R5 was sampled far downstream of the the dye source ($y > 240$ m) where tracer had already spread across the surfzone.
A simple model for a shoreline attached tracer plume is (*Clark et al.*, 2009b)

$$\overline{D}(x, t_{\text{p}}) = \frac{\hat{Q}_0}{\sqrt{4\pi\kappa_{xx}t_{\text{p}}}} \exp\left[\frac{-(x^{-2})}{4\kappa_{xx}t_{\text{p}}}\right], \tag{1}$$

where κ_{xx} is the cross-shore diffusivity, $t_p = y/\bar{V}$ is pseudo-time ($\bar{V}$ is the surfzone-averaged mean alongshore current), and $\hat{Q}_0$ is the normalized flux of (known) tracer input at the source. This model (1) has the cross-shore tracer half-width $\sigma^2_{\text{surf}} = \kappa_{xx}t_p$ growing linearly with time. For

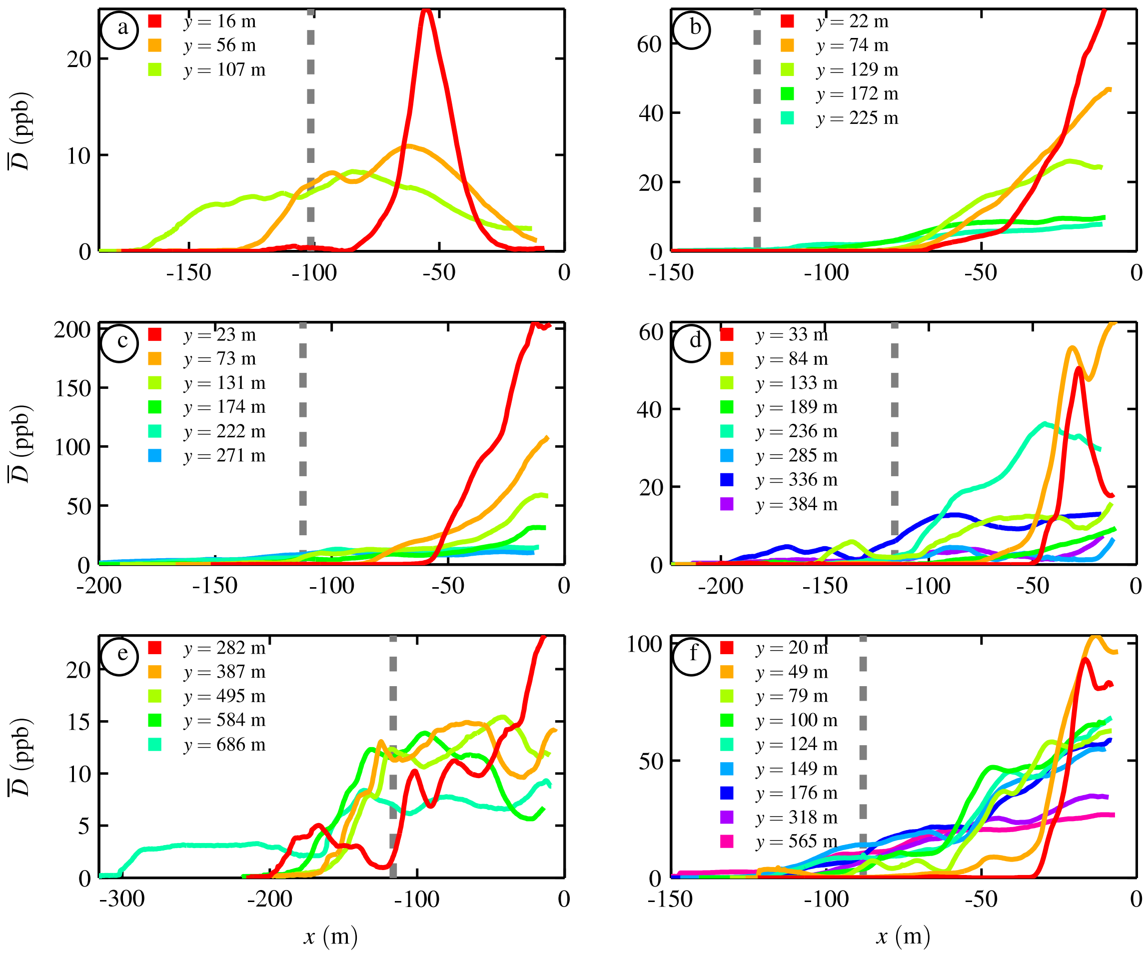

Figure 2: Mean cross-shore tracer concentration $\overline{D}(x, y_j)$ versus x for releases (a) R1, (b) R2, (c) R3, (d) R4, (e) R5, and (f) R6. Colors indicate different downstream alongshore distances y (see legends in each panel). The vertical dashed-gray line represents the outer-limit of the surfzone.

5 of the 6 releases (R5 κ_{xx} could not be estimated), surfzone κ_{xx} (together with error bars) is estimated from the slope of the least squares σ^2_{surf} versus t_{p} fits (*e.g.,* for R6, see Fig. 3). For R1, the κ_{xx} estimation method is modified to account for non-shoreline attached conditions. Only transects where tracer is considered surfzone-contained are used in the fits (*e.g.,* solid black symbols in Fig. 3). Estimated κ_{xx} range from 0.5–$2.5 \pm 0.62\ \mathrm{m^2\,s^{-1}}$. For R6, once the tracer saturates the surfzone, the plume width stops growing (*e.g.,* open symbols in Fig. 3). However, this was not generally observed as jetski transects were not typically driven at such large y (or large t_p). Proposed dye release experiments will include such large downstream sampling.
The simple model (1) predicts for maximum tracer concentration $\overline{D}^{(\mathrm{p})}_{\max} = \hat{Q}_0/(4\pi\kappa_{xx}t_{\mathrm{p}})^{1/2}$ for (near-) shoreline releases. The estimated surfzone κ_{xx} and the known injected dye flux ($\hat{Q}_0$) are used to predict $\overline{D}^{(\mathrm{p})}_{\max}$ for shoreline-attached releases (R2, R3, R4, and R6) when tracer was

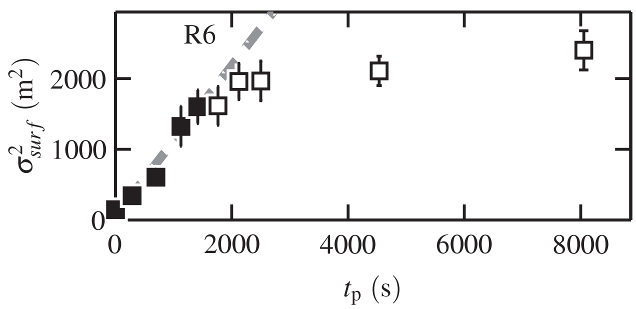

Figure 3: σ^2_{surf} ($\pm$ error-bars) versus t_p for release six (R6). Black symbols indicate observations when tracer was surfzone-contained. Fits to estimate κ_{xx} are indicated with the dashed gray line.

surfzone-contained. The observed $\overline{D}_{\mathrm{max}}$ are consistent with predicted $\overline{D}^{(\mathrm{p})}_{\mathrm{max}}$ (Fig. 4) with high skill (0.72), although the R3 and R6 $\overline{D}^{(\mathrm{p})}_{\mathrm{max}}$ have large errors at the first downstream transect. The linear growth of σ^2_{surf} and the skill in predicting $\overline{D}^{(\mathrm{p})}_{\mathrm{max}}$ indicates that the simple model (1) well represents the surfzone mean tracer plume structure as it is advected downstream. The initial stages of dye dispersion (the near field) and the far downstream are poorly understood.

Two κ_{xx} parameterizations for tracer dispersion were examined by *Clark et al.* (2009b). The first is a breaking-wave (bore) induced mixing scaling where $\kappa_{xx} \sim H_\mathrm{s}^2 T_\mathrm{m}^{-1}$ (*Feddersen*, 2007; *Henderson*, 2007) (H_s is wave height and T_m is wave period). In drifter model simulations (*Spydell et al.*, 2009), horizontal rotational velocities (*i.e.,* vortical flow) generated by finite crest length breaking (*Peregrine*, 1998) or shear instabilities of the alongshore current (*e.g., Oltman-Shay et al.*, 1989) were found to be a primary mixing mechanism. A mixing-length scaling (e.g., *Tennekes and Lumley*, 1972) was examined using a surfzone width L_x length-scale and infragravity horizontal rotational $\overline{\mathcal{V}}_{\mathrm{rot}}$ velocities for a velocity scale, *i.e.,*

$$\kappa_{xx} = \alpha \overline{\mathcal{V}}_{\mathrm{rot}} L_x, \tag{2}$$

where α is a constant expected to be $O(1)$ but < 1. The incident H_s and T_m are used to test the bore induced κ_{xx} scaling. The observed surfzone $\mathcal{V}_{\mathrm{rot}}(x)$ is estimated following *Lippmann et al.* (1999), and the surfzone averaged $\overline{\mathcal{V}}_{\mathrm{rot}}$ range between 0.036-0.09 $\mathrm{m\,s^{-1}}$.

Although observed κ_{xx} generally increase with $H_\mathrm{s}^2\, T_\mathrm{m}^{-1}$ (Fig 5a), the skill is low ($r^2 = 0.32$) and the fit-slope of 11.7 is a factor 6 larger than expected for bore-induced dispersion (*Clark et al.*, 2009b), suggesting that the observed cross-shore dye dispersion is not dominated by the bore-mixing mechanism. The surfzone tracer κ_{xx} increase with $\overline{\mathcal{V}}_{\mathrm{rot}}\, L_x$ (Fig 3b) and the linear best-fit gives an r^2 of 0.59, slope of 0.2, and near-zero y-intercept. The high r^2 and an expected slope < 1 (for a mixing-length scaling) indicate that rotational velocities (surf-zone eddies) play an important role in cross-shore surfzone tracer mixing.

However, only 6 total dye releases were performed at a single beach without significant variation in the wave and current conditions. In addition, the κ_{xx} with overlapping error bars (Fig 5) are not particularly distinct on the different release days. Furthermore, the initial short time (< 100 s or

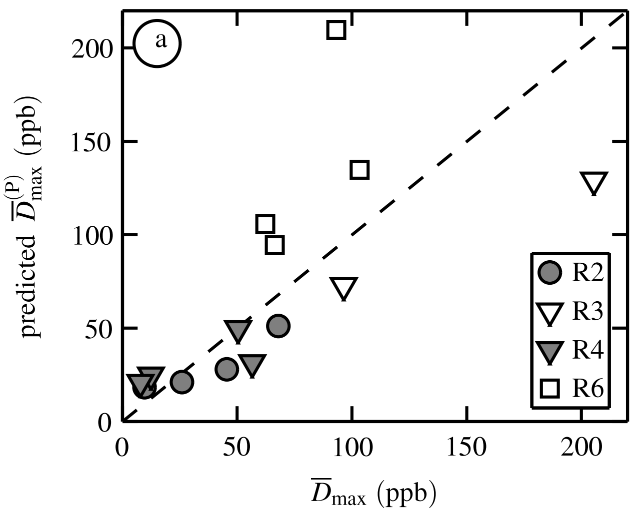

Figure 4: Predicted versus observed $\overline{D}_{\mathrm{max}}$ for shoreline attached releases (R2, R3, R4, R6) and surfzone contained transects. The skill is 0.72.

the near field) cross-shore dispersion of the tracer was not consistently observed and only on two release days were the long time (far field, $y > 500$ m downstream) saturation of the surfzone observed. During HB06, dye was never observed more than 700 m downstream of the dye source. How the tracer evolves and mixes with the waters offshore of the surfzone is totally not understood.

Lastly, the jetski only measures near-surface dye concentrations. For analysis purposes, the dye is assumed to be well mixed (vertically uniform) within the surfzone. Within the surfzone where the depths are shallow (< 3 m) this assumption does not appear to affect cross-shore integrated dye moments (*Clark et al.*, 2009b). However, the validity of this assumption is unknown. The dye tracer that leaks offshore can potentially be concentrated at the surface or at depth. The amount of dye that leaks offshore, it's vertical distribution, and the mechanisms that drive it are unknown.

Surfzone turbulence studies

The turbulent dissipation rate ϵ was significantly larger (by a factor of 10) inside the surfzone (blue curve first 400 hrs) versus seaward of the surfzone (red curve in Fig. 6), indicating the importance of wave breaking to turbulence in the surfzone. The surfzone ϵ is related to the incoming H_{sig} (lower panel Fig. 6) with larger waves leading to larger ϵ. Furthermore, there is significant tidal modulation of surfzone ϵ. At lower tides when the ADV is closer to the surface (and the source of breaking wave turbulence), ϵ is stronger. In addition, at later times (hours 500-700), frame 3 is alternately within and seaward of the surfzone as the tide goes up and down. The frame 3 ϵ varies strongly as wave breaking is turned on and off (see strong oscillations in blue curve in Fig. 6).

We seek a non-dimensional scaling for the dissipation rate ϵ in the surfzone. Following Terray et

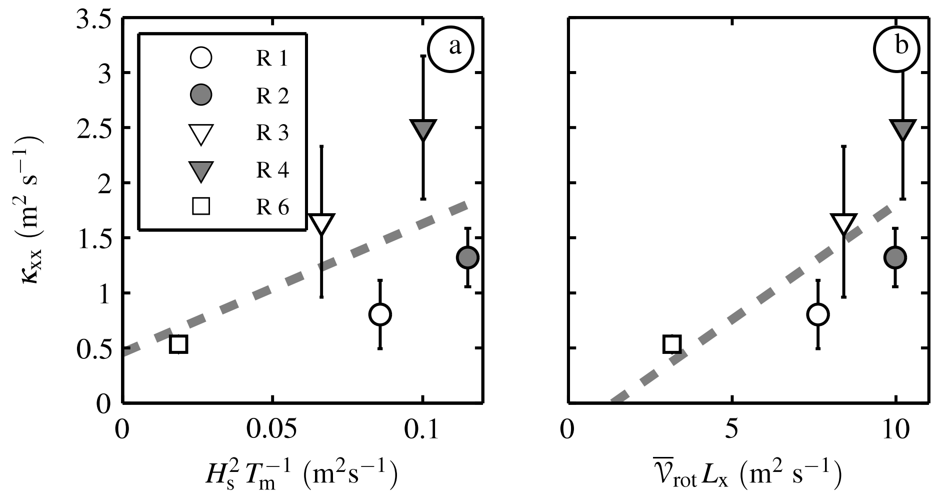

Figure 5: Estimated surfzone cross-shore diffusivity κ_{xx} (with error-bars) versus (a) $H_{\mathrm{sig}}^2\,T^{-1}$ and (b) $\overline{\mathcal{V}}_{\mathrm{rot}}\,L_x$. The fit slopes are 11.7 and 0.2, and r^2 are 0.32 and 0.59 for (a) $H_{\mathrm{sig}}^2\,T^{-1}$ and (b) $\overline{\mathcal{V}}_{\mathrm{rot}}\,L_x$, respectively.

al. (1996), who developed a scaling for open-ocean whitecapping breaking waves, the dissipation is non-dimensionalized as

$$\tilde{\epsilon} = \frac{H_{\mathrm{sig}}\epsilon}{dF/dx} \tag{3}$$

where $dF/dx = d(Ec_g)/dx$ is the cross-shore gradient of the the incoming wave energy flux (Ec_g) which is estimated from the frames. The non-dimensional ϵ has a consistent relationship with the non-dimensional distance below the mean surface z'/H_{sig} at each frame (Fig. 7). This relationship can be modeled as a power law relationship as

$$\frac{H_{\mathrm{sig}}\epsilon}{dF/dx} = C\left(\frac{z'}{H_{\mathrm{sig}}}\right)^{\gamma} \tag{4}$$

where C and γ are fit at each frame.

At the 3 surfzone frames, the fit γ vary between -1.5 and -2 with fit skill varying between 0.4 and 0.6 (Fig. 7). This best-fit γ is consistent with results from open-ocean wave breaking which has $\gamma = -1.9$ (Terray et al., 1996). This implies that the mechanisms by which turbulence diffuses down in the surfzone are similar to those in the open-ocean. However, one open question is why the constant C varies so much between the frames. This is being investigated further.

IMPACT/APPLICATIONS

Potential impacts include improving surfzone and nearshore mixing parameterizations based upon bulk factors such as wave height, wave period, bathymetry, and currents.

RELATED PROJECTS

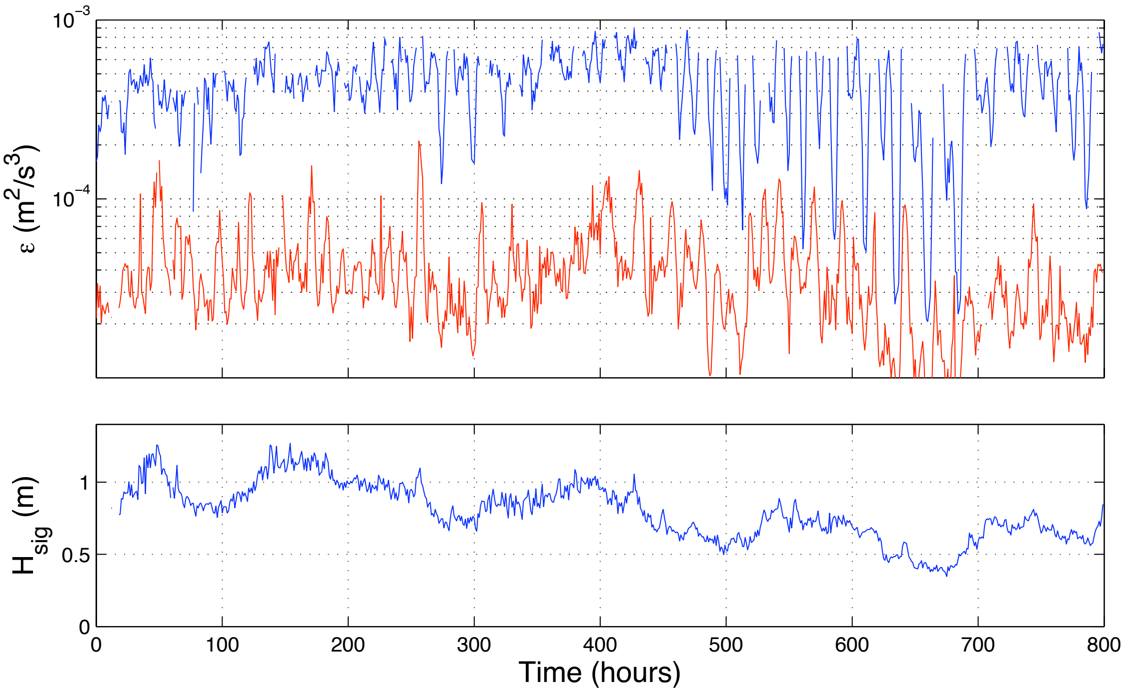

Figure 6: HB06 time series of (top) turbulent dissipation rate ϵ at frames 3 (blue) and 6, and (bottom) incident significant wave height $H_{\rm sig}$ at frame 7.

There are no active related projects.

References

Boehm, A. B., S. B. Grant, J. H. Kim, C. D. McGee, S. Mowbray, C. Clark, D. Foley, and D. Wellmann, Decadal and shorter period variability of surfzone water quality at Huntington Beach, California. *Environ. Sci. Technol.*, *36*, 3885–3892, 2002.

Clark, D. B., F. Feddersen, M. M. Omand, and R. T. Guza, Measuring fluorescent dye in the bubbly and sediment laden surfzone, *Water Air Soil Poll.*, doi: 10.1007/s11270-009-0030-z, 2009a.

Clark, D. B., F. Feddersen, and R. T. Guza, Cross-shore surfzone tracer dispersion in an alongshore current, *J. Geophys. Res.*, submitted, 2009b.

Clarke, L. B., D. Ackerman, and J. Largier, Dye dispersion in the surfzone: Measurements and simple models, *Cont. Shelf Res.*, *27*, 650–669, 2007.

Feddersen, F., Breaking wave induced cross-shore tracer dispersion in the surfzone: Model results and scalings *J. Geophys. Res.*, , **112**, C0912, doi:10.1029/2006JC004006, 2007.

Feddersen, F., Trowbridge, J. H., and Williams, A. J., 2007: Vertical structure of dissipation in the nearshore. *J. Phys. Ocean.*, *37*, 1764–1777.

Haile, R. W., J. S. Witte, M. Gold, R. Cressey, C. D. McGee, R. C. Millikan, A. Glasser, N. Harawa, C. Ervin, P. Harmon, J. Harper, J. Dermand, J. Alamillo, K. Barrett, M. Nides, And

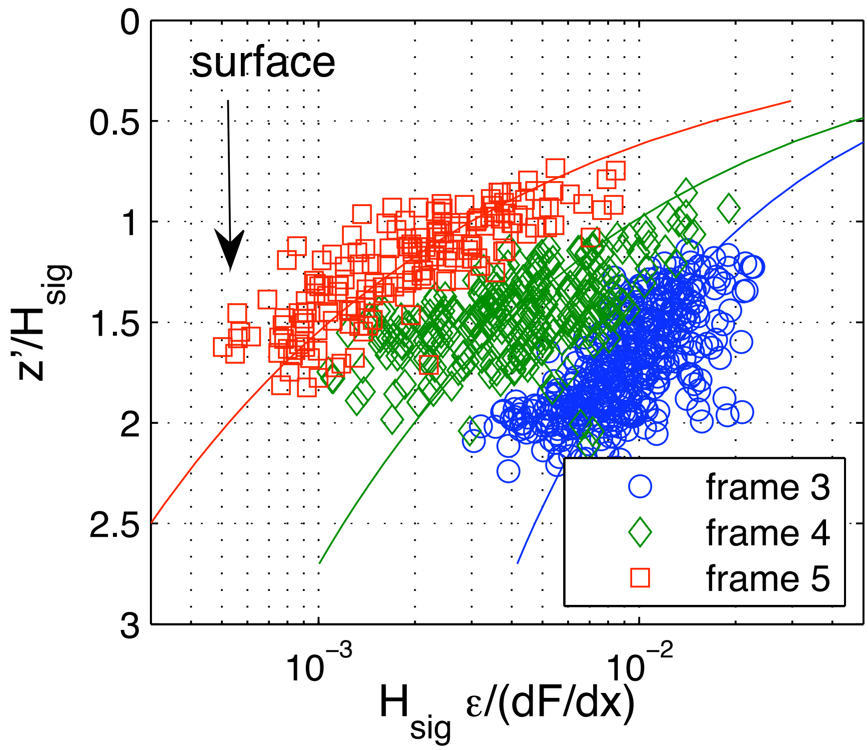

Figure 7: Nondimensional dissipation rate $H_{\text{sig}}\epsilon/(dF/dx)$ against non-dimensional distance below the mean sea-surface z'/H_{sig} at frames 3, 4, and 5 (see legend) when in the surfzone. The solid lines are the best fit to a power law relationship $H_{\text{sig}}\epsilon/(dF/dx) = \alpha(z'/H_{\text{sig}})^{\gamma}$ where $\gamma \approx -1.9$ at all the frames.

G. Wang, The health effects of swimming in ocean water contaminated by storm drain runoff. *Epidemiology*, *10*, 355–363, 1999.

Henderson, S. M., Comment on 'Breaking wave induced cross-shore tracer dispersion in the surfzone: Model results and scalings', *J. Geophys. Res.*, *111*(C12007), doi: 10.1029/2006JC003539, 2007.

Inman, D. L., R. J. Tait, and C. E. Nordstrom, Mixing in the surfzone. *J. Geophys. Res., 26*, 3493–3514, 1971.

Jiang, S. C., and W. Chu, PCR detection of pathogenic viruses in Southern California urban rivers. *J. Applied Microbiology*, *97*, 17–28, 2004.

Lippmann, T. C., T. H. C. Herbers, and E. B. Thornton, Gravity and shear wave contributions to nearshore infragravity motions, *J. Phys. Ocean.*, *29*(2), 231–239, 1999.

Oltman-Shay, J., Howd, P. A., and W. A. Birkemeier, Shear instabilities of the mean longshore current, 2. Field data. *J. Geophys. Res., 94*, 18,031–18,042, 1992

Omand, M., F. Feddersen, D. B. Clark, P. J. S. Franks, J. J. Leichter, and R. T. Guza, The influence of bubbles and sand on chlorophyll fluorescence measurements in the surfzone, *Limnology and Oceanography Methods*, *7*, 354-362, 2009.

Omand, M. O., J. J. Leichter, F. Feddersen, P. J. S. Franks,, and R. T. Guza, Internal wave-driven patches of red tide in the nearshore and surfzone, in preparation for *Limnology and Oceanography*, 2009b.

Peregrine, D., Surf zone currents. *Theor. Comput. Fluid Dyn.*, *10*, 295–309, 1998.

Reeves, R. L., S. B. Grant, R. D. Mrse, C. M. Copil Oancea, B. F. Sanders, A. B. Boehm, Scaling and management of fecal indicator bacteria in runoff from a coastal urban watershed in Southern California. *Environ. Sci. Technol.*, *38*, 2637–2648, 2004.

Spydell, M. S., F. Feddersen, and R. T. Guza, Observations of drifter dispersion in the surfzone: The effect of sheared alongshore currents, *J. Geophys. Res.*, *114*(C07028), doi: 10.1029/2009JC005328, 2009.

Terray, E. A., M. A. Donelan, Y. C. Agrawal, W. M. Drennan, K. K. Kahma, A. J. Williams, and P. Hwang, 1996: Estimates of kinetic energy dissipation under breaking waves. *J. Phys. Oceangr., 26*, 792–807.

Tennekes, H., and J. L. Lumley, *A First Course in Turbulence*, MIT Press, 1972.

PUBLICATIONS

These publications acknowledging ONR support during this support period can be downloaded at http://iod.ucsd.edu/∼falk/papers.html.

- Ladah, L. B., F. Feddersen, G. A. Pearson, and E. A. Serrao, Egg release and settlement patterns of dioecious and hermaphroditic fucoid algae during the tidal cycle, *Marine Biology*, doi:10.1007/s00227-008-1054-42008, 2008.
- Spydell, M. and F. Feddersen, Lagrangian drifter dispersion in the surfzone: Directionally-spread normally incident waves, *J. Phys. Oceangr.,* , **39**, 809-830, DOI: 10.1175/2008JPO3892.1, 2009.
- Clark, D. B., F. Feddersen, M. Omand, and R. T. Guza, A Fluorescent Dye Technique for Measuring Transport and Dispersion in the Surfzone, *Water, Air, Soil Pollution*, DOI: 10.1007/s11270-009-0030-z, 2009.
- Omand, M., F. Feddersen, D. B. Clark, P. J. S. Franks, J. J. Leichter, and R. T. Guza, The influence of bubbles and sand on chlorophyll fluorescence measurements in the surfzone, *Limnology and Oceanography Methods*, **7**, 354-362, 2009.
- Spydell, M., F. Feddersen, and R. T. Guza, Observations of drifter dispersion in the surfzone: The effect of sheared alongshore currents, *J. Geophys. Res.,* , **114**, doi:10.1029/2009JC005328, 2009.
- Clark, D. B., F. Feddersen, R. T. Guza, Cross-shore Surfzone Tracer Dispersion in an Alongshore Current, submitted to *J. Geophys. Res.,* , 2009.